Dalton Transactions

PAPER

Heterobimetallic aluminate derivatives with bulky phenoxide ligands: a catalyst for selective vinyl polymerization†‡

Cite this: DOI: 10.1039/c9dt00761j

Miguel Palenzuela,[a] Mª Teresa Muñoz,[a] Juan F. Vega,[b] Ángel Gutiérrez-Rodríguez,[c] Tomás Cuenca[a] and Marta E. G. Mosquera *[a]

Received 20th February 2019,
Accepted 8th April 2019

DOI: 10.1039/c9dt00761j

rsc.li/dalton

New aluminium-alkali metal heterometallic compounds using the bulky ligand OAr = 2,6-bis(diphenylmethyl)-4-*tert*-butylphenoxide have been synthesized and characterized. The species obtained, [MAlMe$_3$(OAr)] (M = Li(**2a**), Na(**2b**), K(**2c**)) and [MAlMe$_2$(OAr)$_2$] (M = Li(**3a**), Na(**3b**), K(**3c**)), include some of the few heterobimetallic examples of aluminate complexes with O-donor ligands described so far. Their activity in polymerization towards a difunctional monomer, such as Glycidyl Methacrylate (GMA), was evaluated. The compounds were revealed to be able to polymerize the acrylate groups *via* vinyl polymerization. Interestingly, the homometallic counterparts [AlXMe(OAr)] (X = Cl, Me), previously described by us, are very active in ROP processes of GMA. The combined polymerization process using both catalysts has also been explored to obtain a polymeric material with an exciting macromolecular architecture.

Introduction

Within the p-block elements, aluminium is a fascinating metal showing a rich structural chemistry[1] and playing a key role in many catalytic reactions. Aluminium species are active in numerous organic transformations, such as Diels–Alder reactions, cyanosilylation, aldol reactions, alkylations or acylations.[2] In addition, aluminium compounds play a prominent role in many polymerization processes, either as catalysts or co-catalysts.[3] Indeed, the activity of methylaluminoxane as a co-catalyst in olefin polymerization is well known.[4] Moreover, aluminium alkoxide complexes are very good catalysts for ring opening polymerization (ROP) of many oxygenated cyclic molecules such as lactides, lactones and epoxides.[5]

Aluminium *-ate* compounds are exciting species in this area. These heterometallic derivatives contain aluminium in combination with a more electropositive metal, such as an alkali metal, frequently linked *via* a bridging ligand. Many recent studies illustrate the efficient reactivity of *-ate* derivatives in processes such as C–H orthometalation or C–heteroatom bond formation,[6] although their activity in catalytic processes has been less explored.[7] In particular, a few examples have been reported for polymerization reactions, even though, active aluminium–lithium enolate species have been detected in methyl acrylate polymerizations.[8] Furthermore, it has been proposed that lithium–aluminium species with low nuclearity can exert a very good control in the vinyl polymerization of acrylate monomers.[9]

One of our on-going research lines is focused on *-ate* aluminium derivatives with functionalized aryloxide ligands.[10,11] We have reported well-defined heterometallic species containing 2,6-dimethoxyphenoxide ligands that have been shown to be active in methylmetacrylate polymerization.[12] We have extended our studies to bulkier phenols such as 2,6-bis(diphenylmethyl)-4-*tert*-butylphenol[13] aiming to attain heterometallic *-ate* species of lower nuclearity and to study their activity towards the vinyl polymerization of acrylate monomers.

In particular, we have focused our attention on glycidyl methacrylate (GMA), a monomer of industrial interest that presents two functional groups, an acrylate and an oxirane.[14] Monomers such as GMA, with two reactive groups, are very valuable as precursors of functionalized polymers; if only one group is polymerized, the development of catalysts able to selectively polymerize just one functional group is an attractive goal. For GMA, the polymerization of the acrylate group leads to linear poly(glycidylmethacrylate) (PGMA). The most fre-

[a]*Departamento de Química Orgánica y Química Inorgánica, Instituto de Investigacion en Química "Andres M. del Río" (IQAR) Universidad de Alcalá, Campus Universitario, 28871-Alcala de Henares, Madrid, Spain. E-mail: martaeg.mosquera@uah.es*
[b]*BIOPHYM, Department of Macromolecular Physics, Instituto de Estructura de la Materia, IEM-CSIC, C/Serrano 113 bis, 28006 Madrid, Spain*
[c]*Unidad de Difracción de rayos X – Monocristal, Servicios Científico-Técnicos, Universidad de Oviedo, Spain*

† Dedicated to Prof. Pablo Espinet on occasion of this 70th birthday.

‡ Electronic supplementary information (ESI) available. CCDC 1897464–1897467. For ESI and crystallographic data in CIF or other electronic format see DOI: 10.1039/c9dt00761j

quently used method for this vinyl polymerization is a radical mechanism with 2,2′-azobisisobutyronitrile (AIBN) as the initiator.[15] Linear PGMA homopolymers have found applications as column fillings for liquid chromatography,[16,17] coatings, matrix resins, adhesives,[18] drug or gene carriers,[19–21] biosensors,[22] and stabilizers and immobilizers of enzymes.[23] For their part, the polyethers resulting from the ROP reaction of the GMA oxirane group are used as photocurable polymers for electronic devices.[24,25]

In previous investigations, we have studied the polymerization of GMA using the aluminium homometallic derivatives $[AlMeX(OAr)]_n$ bearing the bulky phenoxide ligand 2,6-bis(diphenylmethyl)-4-*tert*-butylphenoxide (OAr). These compounds were extremely active catalysts for the selective ROP of the GMA oxirane group.[26]

In this paper, we report the extension of the studies with the bulky phenol 2,6-bis(diphenylmethyl)-4-*tert*-butylphenol as the ligand precursor for heterometallic *-ate* complexes; this work has led to the isolation of a new family of heterobimetallic species $[MAlMe_{4-x}(OAr)_x]$ (M = Li, Na, K; x = 1, 2). We have also tested the selectivity of these new heterometallic compounds for the polymerization towards the vinyl functionality in the GMA monomer. In addition, we have explored the combined action of the aluminium heterometallic catalysts and their homometallic counterparts, in order to assess their ability to generate novel macromolecular architectures.

Results and discussion

Following the methodology commonly used by our research group,[10–12] the metallated phenol $[M\{2,6\text{-}(CHPh_2)_2\text{-}4\text{-}^tBu\text{-}C_6H_2O\}]_n$ (M = Li, Na, K)[13] was prepared *via* the initial reaction of the phenol with the alkali metal precursor. Further treatment of MOAr with an appropriate aluminium precursor in toluene at −78 °C led to the new heterometallic derivatives in good yields (Scheme 1). Two different types of compounds were obtained depending on the aluminium precursor used. Compounds with stoichiometry $[MAlMe_3(OAr)]$ (**2a–c**) were formed when $AlMe_3$ was the aluminium source, while derivatives $[MAlMe_2(OAr)_2]$ (**3a–c**) were generated if the aluminium precursor was $[AlMe_2(OAr)]_2$.[26]

Compounds **2a–c** and **3a–c** are air sensitive and were stored in a glovebox. They were characterized by analytical and spectroscopic methods. In the ^{1}H-NMR spectra of compounds $[MAlMe_3(OAr)]$ (**2a–c**), the methyl groups bonded to aluminium appear as one singlet that accounts for nine protons at −0.51 (**2a**), −0.39 (**2b**) and −0.32 (**2c**) ppm. For the *tert*-butyl groups, one singlet is observed for **2a** and **2c** (1.09 (**2a**) and 1.12 (**2c**) ppm), while for **2b** two bands at 1.05 and 1.11 are present that integrate for 6 and 3 protons, indicating that one of the methyl groups is in a slightly different environment. The methine atoms appear as one singlet (6.35 (**2a**), 6.48 (**2b**) and 6.53 (**2c**) ppm). Finally, the resonances corresponding to the aromatic ring and the phenyl groups are in the range of 6.89–7.36, 6.96–7.36 and 6.83–7.36 ppm for **2a**, **2b** and **2c**,

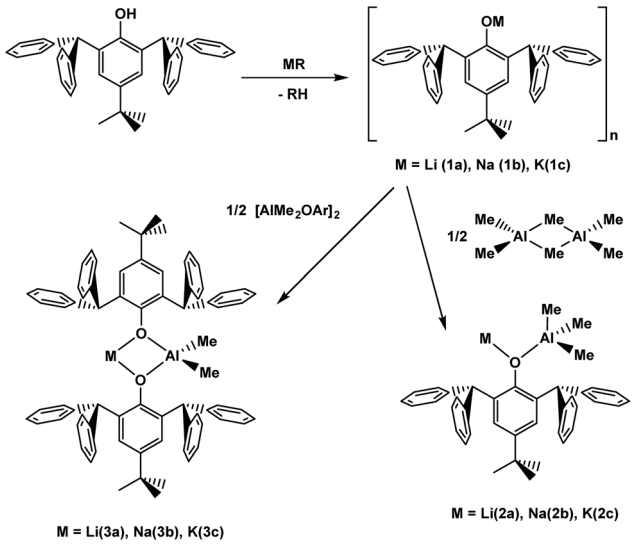

Scheme 1 Synthesis of derivatives **1a–c**, **2a–c** and **3a–c**.

respectively. It is noteworthy that the signal for the methyl groups bonded to the aluminium has similar values for the sodium and potassium compounds, δ −0.39 (**2b**) and −0.32 (**2c**), but moves to more negative resonances for the lithium derivative **2a**. This behaviour indicates a more shielded environment for the methyl groups, which implies that the aluminium atom in **2a** possesses a less acidic character than the sodium and potassium derivatives, which can be attributed to the more covalent character of lithium species.[10,12,27]

In the ^{1}H-NMR spectra of $[MAlMe_2(OAr)_2]$ (**3a–c**), the bands corresponding to the methyl groups bonded to the aluminium appear also as singlets that integrate for six protons. However, in comparison with compounds **2a–c**, there is a surprisingly large shift to lower fields which are located at positive values (0.23 (**3a**), 0.20 (**3b**) and 0.18 (**3c**) ppm). In the analogous family with the 2,6-dimethoxyphenoxyde ligand, a shift in this direction was also observed, as expected since $[MAlMe_2(OAr)_2]$ species may have a more acidic character than $[MAlMe_3(OAr)]$, but the shift occurs to a smaller extent.[10,12] The shift for **3a–c** is so large that it could be attributed to an anisotropic effect caused by the disposition of the phenyl substituents in the aryloxide ligands in relation to the methyl groups. Meanwhile, the corresponding signals for the *tert*-butyl groups (1.04–1.06 ppm), the methine atoms (6.46–6.54 ppm) and the phenyl groups (6.83–7.36 ppm) are in similar ranges to compounds **2a–c**.

Appropriate crystals were isolated from compounds **2a** and **2b** to determine the structure by solid state single-crystal X-ray diffraction. Species **2a** and **2b** are isostructural (Fig. 1 and S5 in the ESI‡). In the asymmetric unit, a heterobimetallic $[MAlMe_3(OAr)]$ unit is present where the bulky phenolate acts as a bridging ligand between the aluminium and the alkali metal. The aluminium centre shows the typical tetrahedral environment and it is bonded to one aryloxide ligand and three methyl groups. The heterobimetallic units are packed in

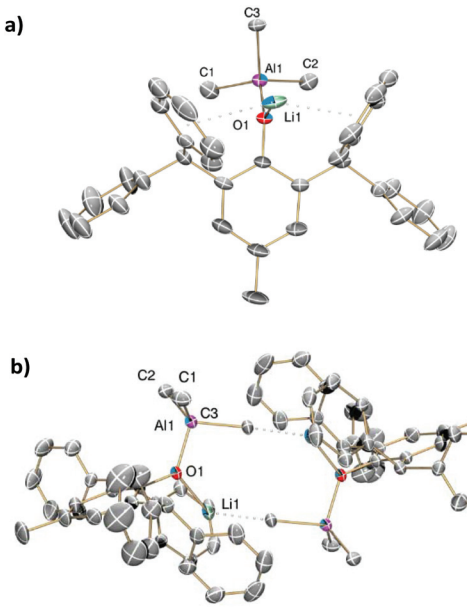

Fig. 1 (a) ORTEP plot of the **2a** asymmetric unit (thermal ellipsoid plots 30% probability). Hydrogen atoms and the methyl groups from the *t*Bu are omitted for clarity. (b) Packing. Selected distances (Å): Al(1)–C(1) 1.978(4), Al(1)–C(2) 1.974(4), Al(1)–C(3) 1.989(3), O(1)–C(41) 1.384(3), O(1)–Li(1) 1.867(7), and Al(1)–O(1) 1.844(2).

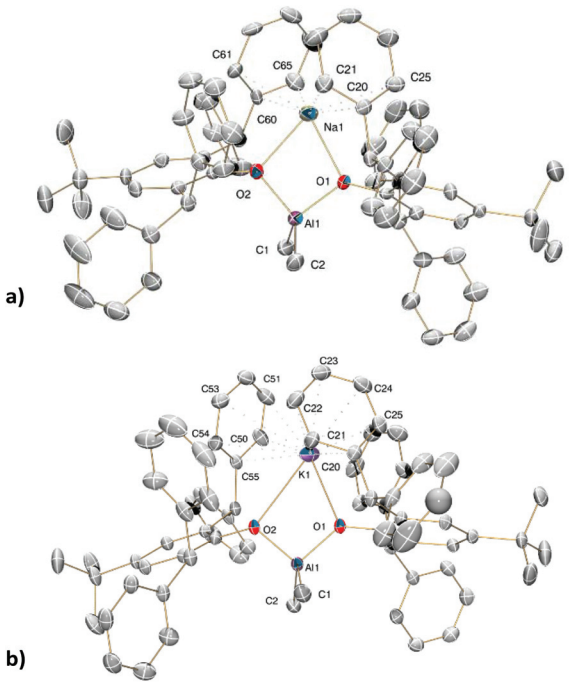

Fig. 2 ORTEP plot (thermal ellipsoid plots 30% probability) of (a) **3b** and (b) **3c**. Hydrogen atoms are omitted for clarity.

pairs as tetrametallic aggregates *via* two Al–Me···M bonds, where the methyl group is bridging the metals. In this way, an eight nuclei ring is generated. The M···Me (M = Li, Na) distances observed (2.258(7) Å (**2a**) and 2.731(3) Å (**2b**)) fall within the range of the few reported examples.[28] The methyl group involved in the interaction suffers from an elongation of the Al–Me distance (Al(1)–C(3) 1.989(3) Å (**2a**) and 2.000(3) Å (**2b**)). In both cases, **2a** and **2b**, the alkali metals are further stabilized by π interactions with two phenyl groups from the *ortho* substituents of the ligand. In fact, the two phenyl rings place themselves in a kind of pocket where the alkali metal fits with an asymmetric coordination, since the distances from the metals to the centroid of the rings are significantly different (3.063(7) Å *vs.* 2.743(7) Å for **2a** and 2.982(3) Å *vs.* 2.727(4) Å for **2b**). In **2a**, the metal shows a η^3-coordination to the closest ring and a η^2-coordination to the other. In **2b**, the coordination could be considered η^3-coordination to both phenyl rings, as a result of the bigger size of the sodium center.

The structure in the solid state of complexes **3b** and **3c** was also determined by single-crystal X-ray diffraction. As shown in Fig. 2, compounds **3b** and **3c** are heterobimetallic, in contrast to the structure observed for the species with the ligand 2,6-dimethoxyphenoxyde. This can be attributed to the high sterical demand of the bulky aryloxide ligand. In **3b** and **3c**, the aluminium centres show a typical tetrahedral environment, being bonded to two aryloxide ligands and two methyl groups. In both cases, **3b** and **3c**, the alkali metals are stabilized by π interactions with two phenyl groups from the ligand substituents. Compound **3b** shows a η^3-coordination to both phenyl rings, while in **3c** the alkali metal has a η^5-coordination to one phenyl ring and a η^6-coordination to the other due to the bigger size of the potassium atom. As observed for compound **2**, the alkali metal fits in the pocket formed by these two phenyl rings. For the sodium atom, the coordination to both rings is asymmetric (2.793(5) Å *vs.* 2.692(8) Å), while for the potassium derivative, **3c**, the asymmetry is observed in the distances to the oxygen atoms of the bridging aryloxide ligands, K1–O1 2.576(2) Å *vs.* K1–O2 2.9625(19) Å (Table 1). This distortion can be attributed to the need for accommodating a big metal ion such as potassium.

Table 1 Selected bond lengths (Å) of **3b** and **3c**

3b			
Na–O1	2.304(4)	Na–O2	2.316(4)
Al1–C1	1.962(5)	Al1–C2	1.938(5)
Al1–O1	1.801(3)	Al1–O2	1.806(3)
O1–C11	1.354(5)	O2–C3	1.365(5)
Na–C20	2.757(5)	Na–C60	2.711(5)
Na–C21	2.814(6)	Na–C61	2.834(5)
Na–C25	3.041(6)	Na–C65	2.884(6)
3c			
K1–O1	2.576(2)	K1–O2	K1–O1
Al1–O1	1.799(2)	Al1–O2	Al1–O1
Al1–C2	1.962(3)	Al1–C1	Al1–C2
O1–C3	1.359(3)	O2–C39	O1–C3
K1···ct1	2.909(3)	K1···ct2	K1···ct1
K1–C50	3.102(3)	K1–C20	3.170(3)
K1–C51	3.334(4)	K1–C21	3.198(3)
K1–C53	3.344(3)	K1–C22	3.237(4)
K1–C54	3.112(3)	K1–C23	3.254(3)
K1–C55	2.970(3)	K1–C24	3.216(3)
		K1–C25	3.170(3)

Table 2 % of error between the theoretical molecular weight and the experimental one

Compound[a]	FW_{exp} (g mol^{-1})	log *D*	FW_t (g mol^{-1})	% error
$[AlLiMe_3(OAr)]$ (**2a**)	587	−9.297	560.31	−4.7%
$[AlNaMe_3(OAr)]$ (**2b**)	552	−9.256	575.97	4.2%
$[AlKMe_3(OAr)]$ (**2c**)	534	−9.306	592.08	9%
$[AlLiMe_2(OAr)_2]$ (**3a**)	981	−9.198	1026.66	4.4%
$[AlNaMe_2(OAr)_2]$ (**3b**)	985	−9.361	1042.71	5.5%
$[AlKMe_2(OAr)_2]$ (**3c**)	1107	−9.419	1058.06	−4.6%

[a] Ar = 2,6-$(CHPh_2)_2$-4-^{t}Bu-C_6H_2. Solvent = C_6D_6.

Remarkably there are very few examples of heterometallic aluminium species with phenoxide ligands with such a low nuclearity.[29,30]

In compounds **3b** and **3c**, the presence of a $\{AlMe_2\{2,6\text{-}(CHPh_2)_2\text{-}4\text{-}^t\text{Bu-}C_6H_2O\}_2\}^-$ moiety is observed. This fragment could be described as a claw that fixes the alkali metals by the phenoxide oxygen atoms while the phenyl groups from the *ortho* substituents help to stabilize the coordination sphere of these metals. When moving from Na to K, this aryloxide fragment does not substantially change the spectroscopic data or its structural parameters, only the dihedral angles between the central AlO_2 core and the aryl rings are modified to accommodate the different alkali ion sizes. This behaviour has been previously reported by our research group for the analogous complexes $[MAlMe_2\{2,6\text{-}(MeO)_2C_6H_3O\}_2]_n$ (M = Li, Na, K)[10] and $[KAlMe_2(PhOH\text{–}CH{=}N\text{–}R)_2]$ (R = C_6H_5, 2,6-^{i}Pr-C_6H_3),[11] where the phenoxide ligands present also groups in *ortho* positions that contribute to grab the alkali metal. The straightforward formation of compounds with this $[MAlMe_2(L)_2]$ (M = Li, Na, K) stoichiometry independently of the nature of the *ortho* substituents could be ascribed to a particular stability of this fragment due to an efficient trapping of the alkali metal.

Since our aim is to study the behaviour of the heterometallic derivatives **2a–c** and **3a–c** as catalysts for polymerization, we also checked their structure in solution. Hence, we have analysed if the nuclearity observed in the solid state was maintained in solution by performing DOSY 2D NMR experiments (NMR spectra in C_6D_6 and the calibration curves can be found in the ESI‡).[31–33] As shown in Table 2, all the compounds are heterobimetallic in solution. The tetrametallic aggregates observed in the solid state for **2a** and **2b** are not present when dissolved in agreement with the singlet observed for the three methyl groups in the NMR spectra.

Polymerization of glycidyl methacrylate (GMA)

Anionic polymerization performed by alkali metal species has been described for acrylic monomers. In particular, heterometallic Al–Li derivatives active in methyl methacrylate polymerization processes have been reported.[8,9,12,34–36] Since GMA has two different functional groups where the polymerization can take place, in our studies with **2a–c** and **3a–c** as catalysts we are interested in checking whether the polymerization would take place *via* the oxirane group, as observed for the homometallic aluminium compounds,[26] or *via* the acrylate group. In the first case, a polyether would be obtained and in the second case, linear PGMA will be the product (Scheme 2). Both polymers can be differentiated by IR spectroscopy, but also by their appearance, since linear PGMA is a white brittle solid, while the polyether obtained from the ROP of the oxirane group is colourless and flexible.

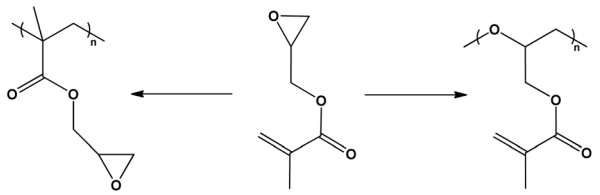

Scheme 2 Polymerization of glycidyl methacrylate by the vinyl group (left) or by the oxirane group (right).

We have carried out our initial studies at different temperatures, but the best results were obtained at 100 °C (see the ESI‡). As shown in Table 3, **2a** gave 85% yield in 30 minutes, while **2b** and **2c** reached higher yields under the same conditions. Moreover, **2b** and **2c** presented 50% yields after only 10 minutes. Hence, the activity of the catalyst is influenced by the alkali metal and increases with the size of the metal, being the lowest for lithium. This behaviour can be attributed to the fact that in compounds **2b** and **2c** the aluminium atom has a stronger acid character than in **2a**, as evidenced in the ^{1}H-NMR spectra. As well, for Na and K the bonding may have a more ionic character which can favour an anionic mechanism. Compounds **3a–c** did not show any activity in this process, most likely due to the unreachability of the alkali metal that prevents the formation of an effective catalytic pair.[37]

The formation of the polymer by means of vinyl polymerization was confirmed by IR spectroscopy. In the spectra, the characteristic signals at 1720 cm^{-1} for the ester, 1130 cm^{-1} for the ether and 903 cm^{-1} for the oxirane groups are observed. However, the corresponding band of the vinyl group at 1638 cm^{-1} has vanished (see the ESI‡). The appearance of the polymer matches with that corresponding to PGMA as well.

The efficiency of the heterometallic compounds for the polymerization of the GMA points towards the acrylate polymerization that can likely take place with the mediation of

Table 3 Results for vinyl polymerization processes of GMA

E	Cat[a]	Mon-cat rate	Yield (%)	*t* (min)
1	**2a**	100-1	85	30
2	**2b**	100-1	50	10
3	**2b**	100-1	>99	30
4	**2c**	100-1	50	10
5	**2c**	100-1	>99	30
6	**3a**	100-1	<0	30
7	**3b**	100-1	<0	30
8	**3c**	100-1	<0	30

[a] Polymerization conditions: 27.86 μmol cat., neat, 100 °C.

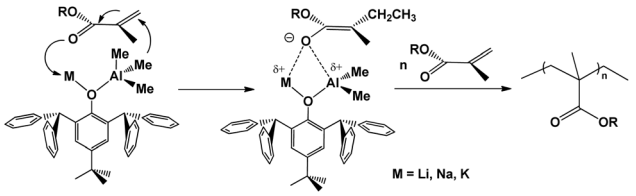

Scheme 3 Proposed mechanism for the acrylate polymerization.

this *-ate* species *via* an anionic mechanism (Scheme 3).[35] This is a different approach than the most common way used for GMA polymerization: RAFT or radical mechanism.[14,15]

When the polymerization is performed using the related homometallic species [AlClMe{2,6-$(CHPh_2)_2$-4-^{t}Bu-C_6H_2O}] as the catalyst, the selective polymerization *via* the oxirane functionality takes place.[26] Thus to complete this study we carried out the combined polymerization using both types of catalysts. Specifically, the ring opening polymerization process was performed first using [AlClMe{2,6-$(CHPh_2)_2$-4-^{t}Bu-C_6H_2O}] as the catalyst, and after 30 minutes at RT, compound **2a** was added and the reaction media were heated at 100 °C for 7 hours. The final polymer was precipitated in hexane and characterized by IR spectroscopy (see the ESI‡). In the IR spectra, the signal at 1720 cm^{-1} for the ester group is observed, while the one at 1657 cm^{-1} has suffered a significant intensity reduction in comparison with that observed in the initial polymer. Moreover, the band at 907 cm^{-1} for the oxirane group is not present. From the IR analysis, it can be inferred that in the new polymer formed, a significant number of the vinyl groups have been polymerized although the complete transformation has not been achieved.

To further explore the features of the new polymer obtained, we performed detailed characterization. Fig. 3 shows the Differential Scanning Calorimetry (DSC) trace of the second heating between −20 °C and 100 °C for the polymer obtained by the combined polymerization process. The typical signature of an amorphous polymer is clearly envisaged from the plot, with a noticeable glass transition at T_g = 11.5 °C (T_{onset} = 7 °C) and a heat capacity jump at this transition of ΔC_p = 0.38 J g^{-1} C^{-1}. The product $T_g \cdot \Delta C_p$ equals to a value of 108.1 (with T_g expressed in K), which is well within the characteristic values reported for most organic glasses and amorphous polymers.[38]

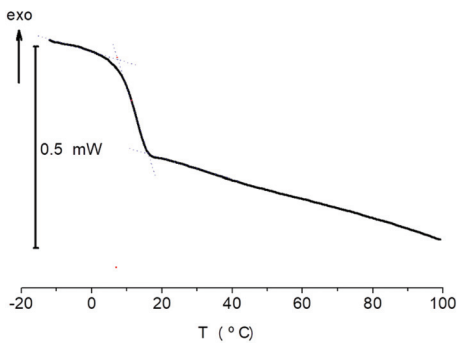

Fig. 3 Second heating DSC trace at 10 °C min^{-1} of the polymer obtained by the combined polymerization.

This result indicates that the synthesized macromolecular assembly is quite flexible at room temperature, an important feature that concerns deformability, processing and uses. However, this value of T_g is significantly higher than the one corresponding to polyether homopolymers obtained from ROP, which has been reported to lie within the range of −40 to −25 °C.[39] The increased T_g in the polymer obtained by the combined polymerization supports the occurrence of the crosslinking among the ROP macromolecular chains, due to a constrained chain mobility induced by covalent bonding. We can imagine the macromolecular assembly as a network of combs created by covalent cross-linking of their backbones, similar to those recently explored by computer simulations and experiments.[40]

We have also explored the macromolecular assembly by Dynamic Light Scattering (DLS) in dilute solution. In Fig. 4a, DLS results are presented as the squared electric field autocorrelation function, $[g_1(t)]^2$, *vs.* time. Due to the polydispersity of the sample, special care should be taken with the data treatment to determine the particle size, so we have applied an inverse Laplace transform by Thikonov analysis to obtain the complete particle size distribution from the autocorrelation function.[41] The intensity averaged peak equals r_h = 23.1 nm. We have also used the size distribution as numbers in order to compare the results with those directly obtained by an Atomic Force Microscopy (AFM) analysis (see below); the number averaged distribution is shown in Fig. 4b. As usual in polydisperse systems, the number average hydrodynamic size is lower than that obtained from the intensity average; r_h = 11.2 nm.[42]

We have additionally studied the morphology of the macromolecular assemblies placed onto a glass surface from a diluted solution using contact mode AFM. The morphological features are clearly observed in Fig. 5a. The macromolecular assemblies have a homogeneous distribution of sizes, but more interestingly they show disk-like thin shapes (few nanometers of height). In fact, it can be suggested that the assemblies exhibit a clear spreading onto the glass surface indicating

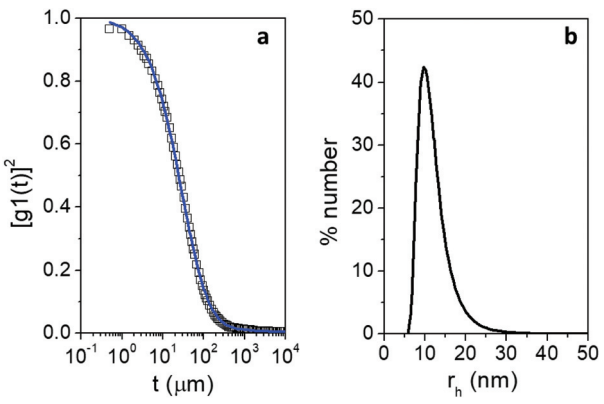

Fig. 4 (a) Squared electric field time autocorrelation function, $[g_1(t)]^2$, of the sample at T = 20 °C *versus* time. The line represents the fit to Thikonov analysis. (b) Number size distribution of the sample studied.

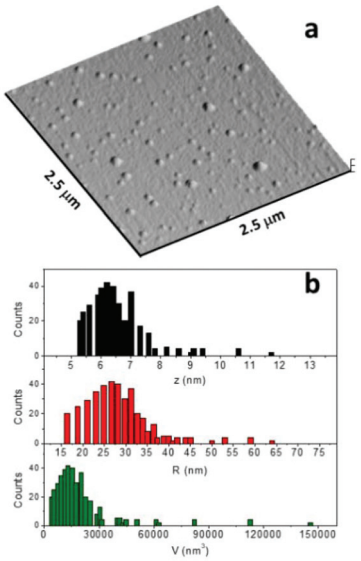

Fig. 5 (a) 3D AFM image of the macromolecular assemblies. (b) Statistical analysis of the macromolecular assemblies.

their flexibility, corresponding to systems above their T_g. Similar results have been recently obtained in lysozyme-dextran nanogels developed for their use as deformable nanocarriers.[43] We have handled our results in a similar way by evaluating 5 μm × 5 μm AFM images using the Gwynddion free software,[44] to obtain the values for the assembly mean height (z), radius (R) and volume (V). The results of the statistical evaluation are shown in Fig. 5b. The average values for the dimensions of the macromolecular assembly obtained from the data are z = 6.5 nm, R = 28.5 nm of radius and V = 11.000 nm^3 (s.d. ± 10%). The relationship obtained between these quantities is characteristic of thin oblate spheroids with the aspect ratio ($p = z/2R$) around $p \sim 0.10$. Interestingly, the average volume measured would give a non-deformed sphere of r_h = 13.8 nm, very close to the hydrodynamic size obtained from the DLS experiments (r_h = 11.5 nm). These results seem to indicate that, in solution, the macromolecular assemblies adopt a nearly 3D spherical shape, but they spread when supported onto the glass surface in the absence of the solvent due to their deformability at room temperature.

This is a new approach to the formation of crosslinked polymers from GMA in a controlled fashion. Crosslinked polymers are of great interest; however in most commercial uses only uncontrolled crosslinking processes are employed, generally *via* photochemical or radical activation. So, the development of strategies that would allow a better control of the process is a very attractive goal.

Experimental

Synthesis

All manipulations were carried out under an inert atmosphere of argon using standard Schlenk and glovebox techniques. All solvents were rigorously dried prior to use following standard methods. NMR spectra were recorded at 400.13 (^{1}H), 155.50 (^{7}Li) and 100.62 (^{13}C) MHz on a Bruker AV400. Chemical shifts (δ) are given in ppm using C_6D_6 as the solvent. ^{1}H and ^{13}C resonances were measured relative to solvent peaks considering TMS δ = 0 ppm, while ^{7}Li was measured relative to external LiCl in D_2O. Elemental analyses were performed on a PerkinElmer Series II 2400 CHNS/O analyzer. IR spectra have been obtained in a PerkinElmer FT-IR Spectrometer Frontier, recording the area between 4000 and 400 cm^{-1}. Samples have been prepared in KBr tablets or in films. Glycidyl Methacrylate was purchased from Aldrich and then purified by vacuum distillation with CaH_2 and stored under argon. All reagents were commercially obtained and used without further purification. Benzyl sodium,[45] Benzyl potassium,[45] $[AlXMe\{2,6\text{-}(CHPh_2)_2\text{-}4\text{-}^t\text{Bu-}C_6H_2O\}]_n$ (X = Me, Cl),[26] 2,6-bis(diphenylmethyl)-4-*tert*-butylphenol[13] and $[M\{2,6\text{-}(CHPh_2)_2\text{-}4\text{-}^t\text{Bu-}C_6H_2O\}]_n$ (M = Li, Na, K)[13] were prepared according to reported methods.

Synthesis of 2a

0.26 mL (0.51 mmol) of $AlMe_3$ 2M were added to a solution of $[Li\{2,6\text{-}(CHPh_2)_2\text{-}4\text{-}^t\text{Bu-}C_6H_2O\}]$ (0.25 g, 0.51 mmol) in 20 mL of toluene at −78 °C. The mixture was stirred for 15 min at −78 °C and then allowed to reach room temperature. The precipitate of a white solid was observed. The suspension was stirred for 2 hours at room temperature and the solid was dissolved after a brief reflux. The solution was stored at −20 °C. After one day, the formation of colourless crystals of compound **2a** was observed. Yield: 85% (0.24 g, 0.43 mmol). NMR: ^{1}H (400 MHz, 293 K, C_6D_6): δ −0.51 (s, 9H, AlCH_3), 1.09 (s, 9H, C(CH_3)$_3$), 6.35 (s, 2H, CH), 6.89–7.36 (Ph + m-OAr–H). ^{13}C-NMR (100.6 MHz, 293 K, C_6D_6): δ −7.08 (s, AlCH$_3$), 31.55 (s, C(CH$_3$)$_3$), 34.34 (s, C(CH$_3$)$_3$), 51.79 (s, CH), 125.70–130.34 (Ph + m-OAr), 133.48 (s, OAr), 134.03 (s, OAr), 134.40 (s, OAr), 137.90 (s, OAr), 145.02 (s, OAr). ^{7}Li-NMR (156 MHz, 293 K, C_6D_6): δ −4.47 (s). Anal. Calc. (%) for $LiAlC_{39}H_{42}O$ (560.67 g mol^{-1}): C, 83.55; H, 7.55. Exp.: C, 83.11; H, 7.73.

Synthesis of 2b

To a solution of $[Na\{2,6\text{-}(CHPh_2)_2\text{-}4\text{-}^t\text{Bu-}C_6H_2O\}]$ (0.26 g, 0.53 mmol) in 20 mL of toluene, 0.26 mL of $AlMe_3$ 2 M (0.53 mmol) were added at −78 °C. The mixture was stirred for 15 min at −78 °C, allowed to reach room temperature and stirred for 2 hours at room temperature. The precipitate of a white solid was observed that was dissolved after a brief reflux. The solution was stored at −20 °C. After one day, colourless crystals of compound **2b** were observed. Yield: 76% (0.23 g, 0.40 mmol). NMR: ^{1}H (400 MHz, 293 K, C_6D_6): δ −0.39 (s, 9H, AlCH_3), 1.05 (s, 3H, C(CH_3)$_3$), 1.11 (s, 6H, C(CH_3)$_3$), 6.48 (s, 2H, CH), 6.96–7.36 (Ph + m-OAr–H). ^{13}C-NMR (100.6 MHz, 293 K, C_6D_6): δ −6.30 (s, AlCH$_3$), 31.08 (s, C(CH$_3$)$_3$), 31.40 (s, C(CH$_3$)$_3$), 51.35 (s, CH), 125.70–129.33 (Ph + m-OAr), 137.90 (s, OAr). Anal. Calc. (%) for $NaAlC_{39}H_{42}O$ (575.97 g mol^{-1}): C, 81.25; H, 7.29. Exp.: C, 80.92; H, 7.52.

Synthesis of 2c

To a solution of [K{2,6-(CHPh$_2$)$_2$-4-^{t}Bu-C$_6$H$_2$O}] (0.30 g, 0.58 mmol) in 20 mL of toluene, 0.29 mL of AlMe$_3$ 2.0 M (0.58 mmol) were added at −78 °C. The mixture was stirred for 15 min at −78 °C and then allowed to reach room temperature. The precipitate of a white solid was observed. The suspension was stirred for 2 hours at room temperature and then the solid was dissolved after a brief reflux. The solution was stored at −20 °C. After one day, a white solid of compound **2c** was observed. The solid was filtered, washed with hexane and dried under vacuum. Yield: 74% (0.23 g, 0.39 mmol). NMR: ^{1}H (400 MHz, 293 K, C$_6$D$_6$): δ −0.32 (s, 9H, AlC*H*$_3$), 1.12 (s, 9H, C(C*H*$_3$)$_3$), 6.53 (s, 2H, C*H*), 6.83–7.36 (Ph + m-OAr–*H*). ^{13}C-NMR (100.6 MHz, 293 K, C$_6$D$_6$): δ −4.99 (s, Al*C*H$_3$), 31.77 (s, C(*C*H$_3$)$_3$), 34.30 (s, *C*(CH$_3$)$_3$), 51.70 (s, *C*H), 125.36–130.42 (Ph + *m*-OAr), 134.79 (s, OAr), 137.90 (s, OAr), 139.63 (s, OAr), 146.53 (s, OAr), 154.90 (s, OAr). Anal. Calc. (%) for KAlC$_{39}$H$_{42}$O (592.08 g mol^{-1}): C, 79.04; H, 7.09. Exp.: C, 78.83; H, 6.68.

Synthesis of 3a

20 mL of toluene were added to a mixture of [Li{2,6-(CHPh$_2$)$_2$-4-^{t}Bu-C$_6$H$_2$O}] (0.29 g, 0.59 mmol) and [AlMe$_2${2,6-(CHPh$_2$)$_2$-4-^{t}Bu-C$_6$H$_2$O}]$_2$ (0.31 g, 0.29 mmol) at −78 °C. The mixture was stirred for 15 min at −78 °C and then allowed to reach room temperature. The yellow solution formed was stirred for 4 hours at room temperature and then the solvent was removed. Compound **3a** was isolated as a pale-yellow solid. Yield: 93% (0.42 g, 0.27 mmol). NMR: ^{1}H (400 MHz, 293 K, C$_6$D$_6$): δ 0.23 (s, 3H, AlC*H*$_3$), 1.06 (s, 9H, C(C*H*$_3$)$_3$), 6.46 (s, 2H, C*H*), 6.87–7.36 (Ph + m-OAr–*H*). ^{13}C-NMR (100.6 MHz, 293 K, C$_6$D$_6$): δ −5.78 (s, Al*C*H$_3$), 31.54 (s, C(*C*H$_3$)$_3$), 34.29 (s, *C*(CH$_3$)$_3$), 50.96 (s, *C*H), 125.70–130.92 (Ph + *m*-OAr), 134.03 (s, OAr), 137.89 (s, OAr), 142.21 (s, OAr), 144.74 (s, OAr), 152.01 (s, OAr). ^{7}Li-NMR (156 MHz, 293 K, C$_6$D$_6$): δ −2.86 (s). Anal. Calc. (%) for LiAlC$_{74}$H$_{72}$O$_2$ (1026.66 g mol^{-1}): C, 86.57; H, 7.01. Exp.: C, 86.69; H, 6.61.

Synthesis of 3b

To a mixture of [Na{2,6-(CHPh$_2$)$_2$-4-^{t}Bu-C$_6$H$_2$O}] (0.094 g, 0.19 mmol) and [AlMe$_2${2,6-(CHPh$_2$)$_2$-4-^{t}Bu-C$_6$H$_2$O}]$_2$ (0.10 g, 92.94 μmol), 10 mL of toluene were added at −78 °C. The mixture was stirred for 15 min at −78 °C and then allowed to reach room temperature. The solution was stirred for 3 hours at room temperature and then the solvent was removed until 4 mL of the solution were left. The mixture was stored at −20 °C; after one week, colourless crystals of compound **3b** were observed. Yield: 78% (0.15 g, 0.15 mmol). NMR: ^{1}H (400 MHz, 293 K, C$_6$D$_6$): δ 0.20 (s, 3H, AlC*H*$_3$), 1.04 (s, 9H, C(C*H*$_3$)$_3$), 6.53 (s, 2H, C*H*), 6.99–7.35 (Ph + m-OAr–*H*). ^{13}C-NMR (100.6 MHz, 293 K, C$_6$D$_6$): δ −5.50 (s, Al*C*H$_3$), 31.57 (s, C(*C*H$_3$)$_3$), 34.26 (s, C(*C*H$_3$)$_3$), 50.78 (s, *C*H), 125.70–129.83 (Ph + *m*-OAr), 133.62 (s, OAr), 137.90 (s, OAr), 141.39 (s, OAr), 143.43 (s, OAr), 145.69 (s, OAr), 153.22 (s, OAr). Anal. Calc. (%) for NaAlC$_{74}$H$_{72}$O$_2$ (1042.71 g mol^{-1}): C, 85.23; H, 6.90. Exp.: C, 85.57; H, 6.45.

Synthesis of 3c

To a mixture of [K{2,6-(CHPh$_2$)$_2$-4-^{t}Bu-C$_6$H$_2$O}] (0.10 g, 96 μmol) and 0.103 g of [AlMe$_2${2,6-(CHPh$_2$)$_2$-4-^{t}Bu-C$_6$H$_2$O}]$_2$ (96 μmol), 10 mL of toluene were added at −78 °C. The mixture was stirred for 15 min at −78 °C and then allowed to reach room temperature. The colourless solution was stirred for 3 hours at room temperature and then the solvent was removed. The white solid obtained corresponded to compound **3c**. Recrystallization in the glovebox in toluene/hexane afforded crystals of enough quality for X-ray diffraction studies. Yield: 75% (0.15 g, 0.14 mmol). NMR: ^{1}H (400 MHz, 293 K, C$_6$D$_6$): δ 0.18 (s, 3H, AlC*H*$_3$), 1.06 (s, 9H, C(C*H*$_3$)$_3$), 6.54 (s, 2H, C*H*), 6.83–7.24 (Ph + m-OAr–*H*). ^{13}C-NMR (100.6 MHz, 293 K, C$_6$D$_6$): δ −4.88 (s, Al*C*H$_3$), 31.63 (s, C(*C*H$_3$)$_3$), 34.25 (s, *C*(CH$_3$)$_3$), 50.77 (s, *C*H), 125.70–130.43 (Ph + *m*-OAr), 133.67 (s, OAr), 137.90 (s, OAr), 140.65 (s, OAr), 143.44 (s, OAr), 146.54 (s, OAr), 154.15 (s, OAr). Anal. Calc. (%) for KAlC$_{74}$H$_{72}$O$_2$ (1058.82 g mol^{-1}): C, 83.93; H, 6.80. Exp.: C, 83.25; H, 7.36.

Single crystal X-ray diffraction of 2a·2C7H8, 2b·2C7H8, 3b·C7H8 and 3c·C7H8

Data collection was performed at 200(2) K, with the crystals covered with perfluorinated ether oil. Single crystals of **2a·2C7H8**, **2b·2C7H8**, **3b·C7H8** and **3c·C7H8** were mounted on a Bruker-Nonius Kappa CCD single crystal diffractometer equipped with graphite-monochromated Mo-Kα radiation (λ = 0.71073 Å). Multiscan[46] absorption correction procedures were applied to the data. The structure was solved using the WINGX package,[47] by direct methods (SHELXS-97) and refined using full-matrix least-squares against F^2 (SHELXL-16 or SHELXL-13).[48] All non-hydrogen atoms were anisotropically refined except for three carbon atoms from the *t*-butyl group in **2a** that are disordered and a disordered toluene molecule in **3c** that were left isotropic. Hydrogen atoms were geometrically placed and left riding on their parent atoms. Two disordered toluene molecules per **2a** and **2b** molecules are present in the unit cell; these solvent molecules were found in the difference Fourier map but were very disordered and it was not possible to get a chemically sensible model for them, so the Squeeze procedure[49] was used to remove their contributions to the structure factors. For **3b**, the crystal quality was poor and diffracted weakly not reaching a Theta(max) value of 25 degrees. Full-matrix least-squares refinements were carried out by minimizing $\sum w(F_o^2 - F_c^2)^2$ with the SHELXL-97 weighting scheme and stopped at shift/err < 0.001. The final residual electron density maps showed no remarkable features. Crystallographic data (excluding structure factors) for the structures reported in this paper have been deposited with the Cambridge Crystallographic Data Centre as supplementary publication no. CCDC 1897464 [**2a·2C7H8**], CCDC 1897465 [**2b·2C7H8**], CCDC 1897466 [**3b·C7H8**] and CCDC 1897467 [**3c·C7H8**].

Differential scanning calorimetry

DSC measurements were performed on Mettler Toledo DSC 3 apparatus. Samples were placed into aluminium crucibles and

measured at temperatures ranging from −20 to 100 °C at heating and cooling rates of 10 °C min^{-1}.

Dynamic light scattering

DLS electric field correlations have been obtained using the Zetasizer Nano ZS (Malvern Instruments, Worcestershire, UK) at T = 20 °C K, and with a 12 μL quartz batch cuvette (ZEN2112). The intensity fluctuations measured are used to produce the scattered intensity time correlation function, $g_2(\tau)$. The time-dependence autocorrelation function was acquired in chloroform solutions of the sample at a weight fractional concentration of 10^{-6}, every 10 s, with 15 acquisitions for each run. The sample solution was illuminated by using a λ_0 = 633 nm laser at a constant power, and the intensity of light scattered at an angle of θ = 173° was measured by using an avalanche photodiode.

Atomic force microscopy

AFM analysis was carried out in a μTA™ 2990 Micro-Thermal Analyzer (TA Instruments, Inc., New Castle, DE, USA). The analysis was performed on samples prepared by deposition of a drop of the dilute sample solution in chloroform onto glass wafers and the solvent was left to evaporate for 24 hours. Topography images were obtained in the contact mode. A V-shaped silicon nitride probe with a cantilever length of 200 μm and a spring constant of 0.032 N m^{-1} was used. The size of the images was 10 and 5 μm^2.

Conclusions

New aluminate alkali metal derivatives [$MAlMe_3${2,6-$(CHPh_2)_2$-4-^{t}Bu-C_6H_2O}] (M = Li(**2a**), Na(**2b**), K(**2c**)) and [$MAlMe_2${2,6-$(CHPh_2)_2$-4-^{t}Bu-C_6H_2O}$_2$] (M = Li(**3a**), Na(**3b**), K(**3c**)) have been synthesized and characterized. These compounds are active catalysts for the vinyl polymerization of glycidyl methacrylate (GMA). Considering that the aluminium homometallic counterparts [$AlClMe${2,6-$(CHPh_2)_2$-4-^{t}Bu-C_6H_2O}], previously described by us, polymerize selectively the GMA oxirane group *via* ROP, we combined the action of both catalysts to generate a new polymeric material. The macromolecule obtained shows remarkable properties, such as it is composed of flexible particles, bigger than 10 nm, that are spheres in solution but flattened when deposited on glass.

Herein we have reported an interesting approach that allows the controlled polymerization of the two functional groups present in a difunctional monomer such as GMA to give macromolecular architectures with remarkable properties. Considering the wide use of GMA derived polymers as carriers in biological applications, the possibility of preparing units of controlled structures that can also be functionalized opens an exciting prospect.

Conflicts of interest

There are no conflicts to declare.

Acknowledgements

Financial support from Spanish Government (MINECO CTQ2014-58270-R), the Alcalá University, Spain (CCG2015/EXP-039) and EU COST Action CA15106 (CHAOS) is gratefully acknowledged. Dr M. T. M. thanks the Universidad de Alcalá and Comunidad de Madrid for a Postdoctoral Research Contract. M. P. thanks the Universidad de Alcalá for a Predoctoral Fellowship.

Notes and references

1 M. Witt and H. W. Roesky, *Curr. Sci.*, 2000, **78**, 410; S. Saito, Aluminum, in *Comprehensive Organometallic Chemistry III*, ed. R. H. Crabtree and D. M. P. Mingos, Elsevier, Oxford, 2007, vol. 9, p. 245.

2 U. Pindur, G. Lutz and C. Otto, *Chem. Rev.*, 1993, **93**, 741; M. Brasse, J. Cámpora, M. Davies, E. Teuma, P. Palma, E. Álvarez, E. Sanz and M. L. Reyes, *Adv. Synth. Catal.*, 2007, **349**, 2111; M. P. Shaver, L. E. N. Allan and V. C. Gibson, *Organometallics*, 2007, **26**, 2252; J. Zhao, H. B. Song and C. M. Cui, *Organometallics*, 2007, **26**, 1947; W. Li, X. Ma, M. G. Walawalkar, Z. Yang and H. V. Roesky, *Coord. Chem. Rev.*, 2017, **35**, 14; T. Taguchi and H. Yanai, *Acid Catal. Mod. Org. Synth.*, 2008, **1**, 241.

3 S. Dagorne and C. Fliedel, Organoaluminum Species in Homogeneous Polymerization Catalysis, in *Modern Organoaluminum Reagents: Preparation, Structure, Reactivity and Use*, ed. S. Woodward and S. Dagorne, Springer, Heidelberg, 2013, p. 125.

4 H. Sinn and W. Kaminsky, *Adv. Organomet. Chem.*, 1980, **18**, 99; H. Sinn, W. Kaminsky, H. J. Vollmer and R. Woldt, *Angew. Chem., Int. Ed. Engl.*, 1980, **19**, 390; E. Y. X. Chen and T. J. Marks, *Chem. Rev.*, 2000, **100**, 1391; E. Zurek and T. Ziegler, *Organometallics*, 2002, **21**, 83.

5 G. Martínez, S. Pedrosa, V. Tabernero, M. E. G. Mosquera and T. Cuenca, *Organometallics*, 2008, **27**, 2300; O. Dechy-Cabaret, B. Martin-Vaca and D. Bourissou, *Chem. Rev.*, 2004, **104**, 6147; N. Spassky, M. Wisniewski, C. Pluta and A. LeBorgne, *Macromol. Chem. Phys.*, 1996, **197**, 2627; N. Nomura, R. Ishii, M. Akakura and K. Aoi, *J. Am. Chem. Soc.*, 2002, **124**, 5938; S. Dagorne, M. Bouyahyi, J. Vergnaud and J. F. Carpentier, *Organometallics*, 2010, **29**, 1865; P. Hormnirun, E. L. Marshall, V. C. Gibson, A. J. P. White and D. J. Williams, *Am. Chem. Soc.*, 2004, **126**, 2688; K. Press, I. Goldberg and M. Kol, *Angew. Chem., Int. Ed.*, 2015, **54**, 14858; P. McKeown, M. G. Davidson, G. Kociok-Kohn and M. D. Jones, *Chem. Commun.*, 2016, **52**, 10431; C. Kan, J. Ge and H. Ma, *Dalton Trans.*, 2016, **45**, 6682; T. M. Ovitt and G. W. Coates, *J. Am. Chem. Soc.*, 2002, **124**, 1316; M. Bouyahyi, E. Grunova, N. Marquet, E. Kirillov, C. M. Thomas, T. Roisnel and J. F. Carpentier, *Organometallics*, 2008, **27**, 5815; D. Pappalardo, L. Annunziata and C. Pellecchia, *Macromolecules*, 2009, **42**,

6056; D. J. Darensbourg, O. Karroonnirun and S. J. Wilson, *Inorg. Chem.*, 2011, **50**, 6775.
6 R. E. Mulvey, F. Mongin, M. Uchiyama and Y. Kondo, *Angew. Chem., Int. Ed.*, 2007, **46**, 3802; M. Uzelac and E. Hevia, *Chem. Commun.*, 2018, **54**, 2455; A. Krasovskiy and P. Knochel, *Angew. Chem., Int. Ed.*, 2004, **43**, 3333; B. Haag, M. Mosrin, H. Ila, V. Malakhov and P. Knochel, *Angew. Chem., Int. Ed.*, 2011, **50**, 9794; E. Hevia, J. Z. Chua, P. Garcia-Alvarez, A. R. Kennedy and M. D. McCall, *Proc. Natl. Acad. Sci. U. S. A.*, 2010, **107**, 5294; C. Vidal, J. García-Alvarez, A. Hernán-Gómez, A. R. Kennedy and E. Hevia, *Angew. Chem., Int. Ed.*, 2014, **53**, 5969; H. Naka, J. V. Morey, J. Haywood, D. J. Eisler, M. McPartlin, F. Garcia, H. Kudo, Y. Kondo, M. Uchiyama and A. E. H. Wheatley, *J. Am. Chem. Soc.*, 2008, **130**, 16193.
7 V. A. Pollard, S. A. Orr, R. McLellan, A. R. Kennedy, E. Hevia and R. E. Mulvey, *Chem. Commun.*, 2018, **54**, 1233; Y. Hua, Z. Guo, H. Han and X. Wei, *Organometallics*, 2017, **36**, 877; C. Decu, C. Casey, M. C. Case and A. J. Shusterman, *Organometallics*, 2012, **31**, 7849; M. J. Harvey, M. Proffitt, P. Wei and D. A. Atwood, *Chem. Commun.*, 2001, 2094; S. Singh, J. Chai, A. Pal, V. Jancik, H. W. Roesky and R. Herbst-Irmer, *Chem. Commun.*, 2007, 4934; T. Arai, H. Sasai, K.-i. Aoe, K. Okamura, T. Date and M. Shibasaki, *Angew. Chem., Int. Ed. Engl.*, 1996, **35**, 104.
8 A. Rodriguez-Delgado and E. Y. X. Chen, *J. Am. Chem. Soc.*, 2005, **127**, 961.
9 E. Y. X. Chen, *Chem. Rev.*, 2009, **109**, 5157; R. J. Peace, M. J. Horton, G. L. N. Peron and A. B. Holmes, *Macromolecules*, 2001, **34**, 8409; B. Lian, C. M. Thomas, O. L. Casagrande Jr., C. W. Lehmann, T. Roisnel and J. F. Carpentier, *Inorg. Chem.*, 2007, **46**, 328.
10 M. T. Munoz, T. Cuenca and M. E. G. Mosquera, *Dalton Trans.*, 2014, **43**, 14377; M. T. Munoz, G. Barandika, B. Bazan, T. Cuenca and M. E. G. Mosquera, *Eur. J. Inorg. Chem.*, 2017, **2017**, 1994.
11 F. M. Garcia-Valle, V. Tabernero, T. Cuenca, J. Cano and M. E. G. Mosquera, *Dalton Trans.*, 2018, **47**, 6499; M. Fernandez-Millan, M. Temprado, J. Cano, T. Cuenca and M. E. G. Mosquera, *Dalton Trans.*, 2016, **45**, 10514.
12 M. T. Munoz, C. Urbaneja, M. Temprado, M. E. G. Mosquera and T. Cuenca, *Chem. Commun.*, 2011, **47**, 11757.
13 K. Searles, B. L. Tran, M. Pink, C. H. Chen and D. J. Mindiola, *Inorg. Chem.*, 2013, **52**, 11126.
14 S. Jiang, J. Ling, J. Nie, Z. Meng, M. Wang, Q. Yu and K. Wang, *J. Polym. Mater.*, 2016, **33**, 469; I. Erol, D. N. Devrim, H. Ciftci, B. Ersoy and I. H. Cigerci, *J. Macromol. Sci., Part A: Pure Appl. Chem.*, 2017, **54**, 434.
15 S. U. Celik and A. Bozkurt, *Eur. Polym. J.*, 2007, **44**, 213.
16 R. Linda, L. W. Lim and T. Takeuchi, *Anal. Sci.*, 2013, **29**, 631.
17 S. Yang, F. Ye, Q. Lv, C. Zhang, S. Shen and S. Zhao, *J. Chromatogr. A*, 2014, **1360**, 143.
18 S. Ghosh and N. Krishnamurti, *Eur. Polym. J.*, 2000, **36**, 2125.
19 M. Bagheri and F. Motirasoul, *e-Polymers*, 2012, **12**, 1003.
20 W. Xun, Y. Yi, C. Zhang and S. Zheng, *J. Macromol. Sci., Part A: Pure Appl. Chem.*, 2013, **50**, 399.
21 Q. L. Li, W. X. Gu, H. Gao and Y. W. Yang, *Chem. Commun.*, 2014, **50**, 13201.
22 S. K. Ozoner, E. Erhan, F. Yilmaz, P. Ergenekon and I. Anil, *J. Chem. Technol. Biotechnol.*, 2013, **88**, 727.
23 C. Li, Y. Lou, Y. Wan, W. Wang, J. Yao and B. Zhang, *Water Sci. Technol.*, 2013, **67**, 2287.
24 N. Bicak and B. Karagoz, *Polym. Bull.*, 2006, **56**, 87.
25 B. Karagoz and N. Bicak, *Eur. Polym. J.*, 2007, **44**, 106.
26 M. T. Munoz, M. Palenzuela, T. Cuenca and M. E. G. Mosquera, *ChemCatChem*, 2018, **10**, 936.
27 C. Schwarz, L. T. Scharf, T. Scherpf, J. Weismann and V. H. Gessner, *Chem. – Eur. J.*, 2019, **21**, 2793.
28 G. Schnee, O. N. Faza, D. Specklin, B. Jacques, L. Karmazin, R. Welter, C. S. Lopez and S. Dagorne, *Chem. – Eur. J.*, 2015, **21**, 17959; S. R. Boss, M. P. Coles, R. Haigh, P. B. Hitchcock, R. Snaith and A. E. H. Wheatley, *Angew. Chem., Int. Ed.*, 2003, **42**, 5593; M. Niemeyer and P. P. Power, *Organometallics*, 1995, **14**, 5488; H. Naka, M. Uchiyama, Y. Matsumoto, A. E. H. Wheatley, M. McPartlin, J. V. Morey and Y. Kondo, *J. Am. Chem. Soc.*, 2007, **129**, 1921; D. R. Armstrong, R. P. Davies, D. J. Linton, R. Snaith, P. Schooler and A. E. H. Wheatley, *J. Chem. Soc., Dalton Trans.*, 2001, 2838; M. D. Fryzuk, G. R. Giesbrecht and S. J. Rettig, *Organometallics*, 1997, **16**, 725; A. Hernan-Gomez, A. Martin, M. Mena and C. Santamaria, *Dalton Trans.*, 2013, **42**, 5076; J. M. Cole, P. G. Waddell, A. E. H. Wheatley, G. J. McIntyre, A. J. Peel, C. W. Tate and D. J. Linton, *Organometallics*, 2014, **33**, 3919; F. Pourpoint, Y. Morin, R. M. Gauvin, J. Trebosc, F. Capet, O. Lafon and J.-P. Amoureux, *J. Phys. Chem. C*, 2013, **117**, 18091; S. R. Boss, J. M. Cole, R. Haigh, R. Snaith, A. E. H. Wheatley, G. J. McIntyre and P. R. Raithby, *Organometallics*, 2004, **23**, 4527; D. R. Armstrong, W. Clegg, R. P. Davies, S. T. Liddle, D. J. Linton, P. R. Raithby, R. Snaith and A. E. H. Wheatley, *Angew. Chem., Int. Ed.*, 1999, **38**, 3367.
29 W. Clegg, E. Lamb, S. T. Liddle, R. Snaith and A. E. H. Wheatley, *J. Organomet. Chem.*, 1999, **573**, 305; A. G. Avent, C. Eaborn, I. B. Gorrell, P. B. Hitchcock and J. D. Smith, *J. Chem. Soc., Dalton Trans.*, 2002, 3971.
30 H. Noth, A. Schlegel, J. Knizek, I. Krossing, W. Ponikwar and T. Seifert, *Chem. – Eur. J.*, 1998, **4**, 2191; M. B. Power, S. G. Bott, J. L. Atwood and A. Barron, *J. Am. Chem. Soc.*, 1990, **112**, 3446.
31 A. K. Rogerson, J. A. Aguilar, M. Nilsson and G. A. Morris, *Chem. Commun.*, 2011, **47**, 7063.
32 D. Li, G. Kagan, R. Hopson and P. G. Williard, *J. Am. Chem. Soc.*, 2009, **131**, 5627.
33 D. Li, I. Keresztes, R. Hopson and P. G. Williard, *Acc. Chem. Res.*, 2009, **42**, 270.
34 M. Tabuchi, T. Kawauchi, T. Kitayamaand and K. Hatada, *Polymer*, 2002, **43**, 7185; T. Kitayama, Y. Zhang and K. Hatada, *Polym. Bull.*, 1994, **32**, 439.

35 T. Kitaura and T. Kitayama, *Macromol. Rapid Commun.*, 2007, **28**, 1889; T. Kitaura and T. Kitayama, *Polym. J.*, 2013, **45**, 1013.
36 H. Schlaad, B. Schmitt, A. H. E. Mueller, S. Juengling and H. Weiss, *Macromolecules*, 1998, **31**, 573.
37 Y. Ning, H. Zhu and E. Y. X. Chen, *J. Organomet. Chem.*, 2007, **692**, 4535.
38 R. Simha and R. F. Boyer, *J. Chem. Phys.*, 1962, **37**, 1003.
39 A. Labbe, A. L. Brocas, E. Ibarboure, T. Ishizone, A. Hirao, A. Deffieux and S. Carlotti, *Macromolecules*, 2011, **44**, 6356.
40 H. Liang, Z. Cao, Z. Wang, S. S. Sheiko and A. V. Dobrynin, *Macromolecules*, 2017, **50**, 3430; H. Liang, S. S. Sheilko and A. V. Dobrynin, *Macromolecules*, 2018, **51**, 638; H. Liang, B. J. Morgan, G. Xie, M. R. Martinez, E. B. Zhulina, K. Matyjaszewski, S. S. Sheiko and A. V. Dobrynin, *Macromolecules*, 2018, **51**, 10028.
41 S. W. Provencher, *Comput. Phys. Commun.*, 1982, **27**, 213.
42 L. H. Hanus and H. J. Ploehn, *Langmuir*, 1999, **15**, 3091.
43 J. M. Myerson, B. Braender, O. Mcpherson, P. M. Glassman, R. Y. Kiseleva, V. V. Shuvaev, O. Marcos-Contreras, M. E. Grady, H. S. Lee, C. F. Greineder, R. V. Stan, R. J. Composto, D. M. Eckmann and V. R. Muzykantov, *Adv. Mater.*, 2018, **30**, 1802373.
44 D. Necas and P. Klapetek, *Cent. Eur. J. Phys.*, 2012, **10**, 181.
45 L. Lochmann, J. Pospisil and D. Lim, *Tetrahedron Lett.*, 1966, **7**, 257.
46 R. H. Blessing, *Acta Crystallogr., Sect. A: Found. Crystallogr.*, 1995, **51**, 33.
47 L. J. Farrugia, *J. Appl. Crystallogr.*, 1999, **32**, 837.
48 G. M. Sheldrick, *Acta Crystallogr., Sect. A: Found. Crystallogr.*, 2008, **64**, 112; G. M. Sheldrick, *Acta Crystallogr., Sect. C: Struct. Chem.*, 2015, **71**, 3–8.
49 P. Van der Sluis and A. L. Spek, *Acta Crystallogr., Sect. A: Found. Crystallogr.*, 1990, **A46**, 194.